

# Monitoring Nonlinearities and Power Smoothing in Modified Mathematical Modeled Type-III Wind Turbine System using Artificial Neural Network

Bibhu Prasad Ganthia<sup>1\*</sup>, Shilpa Patra<sup>1</sup>, Binodinee Swain<sup>1</sup>, Monalisa Mohanty<sup>2</sup>, Sunita Pahadasingh<sup>3</sup>

Assistant Professor, Department of Electrical Engineering, Indira Gandhi Institute of Technology, Sarang, Dhenkanal, Odisha, India, 759146<sup>1</sup>

Research Associate, Department of Electrical and Electronics Engineering, Siksha 'O' Anusandhan Deemed to be University, Bhubaneswar, Odisha, India, 751030<sup>2</sup>

Assistant Professor, Department of Electrical Engineering, Odisha University of Technology & Research (Formerly CET), Bhubaneswar, Odisha, India, 751003<sup>3</sup>

## Abstract

*For feasible wind power generation the speed of the rotor should be maintained balanced with respect to the production of generator power. This research introduces a sliding mode controller to manage wind speed and preserve system stability. It is useful to reduce the nonlinearities using an Artificial Neural Network based Radial Basis Function Neural Network (RBFN). The tip speed ratio technique is utilized in this paper to harvest the most power from wind energy. To optimize this Tip Speed Ratio (TSR) approach, a Proportional-Integral PI-RBFN tuned sliding mode controller was employed to obtain maximum power while minimizing active power losses. Nonlinearities in the pitch angle due to variable wind speed can be solved using this proposed technique. Hence in this paper the robustness of the modified Type-III wind turbine system is studied using MATLAB Simulink. The Simulink results are compared with the existing technique of Double Fed Induction Generator (DFIG) based modified Type-III wind turbines.*

## Keywords

*Wind energy, Type III Wind Turbine, Wind Speed, Pitch Angle Control, RBFN, Sliding Mode Control, Power Smoothing.*

## 1. Introduction

Wind energy, being a renewable source of energy, is now in high demand across all power sectors due to its clean and abundant nature. It could be critical in balancing power demand and increasing energy efficiency for business and residential utilities [1]. The best part about this type of energy is that it does not pollute the environment by generating toxic gases. As a result, it is employed to meet our energy needs as a useful source of energy. To attain high output, a balanced and dependable power system with complete control is essential [2]. Renewable energy sources are becoming increasingly crucial in the huge Generation, Transmission and Distribution system's balancing [3]. We now produce 15 to 20 million Megawatt of power from renewable sources, with wind being the most cost-effective [4]. This can be utilized in both independent and grid-integrated modes to balance out power needs. For complete control over power generation, transmission and distribution, a technical wind turbine system requires both mechanical and electrical components. We started with double fed induction generators, which have no control mechanism and generate losses owing to abrupt variations in wind speed because they are designed for fixed speed operation [1] [16]. Later on we developed the type-III wind turbine system which uses DFIGs with full control over speed and power generation. These are designed with Rotor side and grid side converter based with Maximum power point tracking abilities. Then type-IV PMSG based but the cost is so high, these mechanisms are less used in the world. In our country India type –III DFIGs are maximum used and play efficient power generations in both standalone and grid connected mode. But the controller to the rotor side and grid side should be more precise and faster responsive techniques should be implemented. Many researchers are using adaptive techniques like genetic algorithms, Artificial intelligence and meta-heuristic controllers for fault analysis during transients [1][2]. Fuzzy logic controllers are another example of a control approach that can be used to provide a quicker response to transients. Because the wind energy system requires a steady wind speed for reliable power generation, the wind speed should be balanced between low and high speeds. Wind flow might be unpredictable, causing harm to the system, so the controllers for the rotor and grid should be thoroughly evaluated and implemented [2] [3].

## 2. Literature Survey

The Lyapunov-based sliding mode control (SMC) approach has a number of advantages over previous approaches. For many practical systems, it has been recognized as one of the most effective design methodologies [1][4]. It may be used to tackle issues that are both linear and nonlinear. It may be used for both continuous-time and discrete-time systems, and it has long been regarded as a reliable control system approach due to its simple design procedure and robustness to system uncertainties and external disturbances. SMC's purpose is to transfer a system route's state to an appropriate area in a finite period of time and keep it there. After that, the problem region is labeled as a sliding surface or switching, implying that the system state variables are related. [3][5] It is completely defined by a differential equation that defines the dynamics of the system. Dynamic sliding mode describes the system's behavior as it moves across the sliding surface. Chattering, a type of high-frequency oscillation that can cause system instability and damage, is one of the most common and major undesirable phenomena that SMCs experience. SMC was used in this work to control and regulate nonlinearities in order to get the most power out of it [6][13][15]. The adaptive

techniques can be used with the sliding mode controller technique to improve power smoothing under variable wind speeds. The pitch angle control can be improved using genetic algorithm optimization techniques. Considering wind turbulence and disturbances this paper can be helpful to enhance the tuning process using radial basis function neural networks. The modified rotor based type-III wind turbine used in this paper where the proposed techniques are implemented. Different operating modes were used previously to improve the wind power generation by controlling the wind speeds. The Radial Basis Function Network approach, which is employed in type-III wind turbine systems, can be used to minimize nonlinearities. The particle swarm optimization technique was utilized to optimize the wind power generation's steady state and transient characteristics. The RBFN technique is combined with the sliding mode control technique in this research. This study aids in the reduction of pitch angle rotational error and the enhancement of transient stability. Bode Plots and Nyquist Plots are used to validate the system's stability under transients and wind speed disturbances. In the findings section, where the comparisons are shown, the power generation from this simulation study is shown. This study also emphasizes power smoothing by avoiding active power loss and reactive power compensation [10-14].

### 3. Methods

#### 3.1 Wind Energy Conversion Systems

Sunlight is the reason for atmospheric heating which causes the wind to flow. In hot and cold regions due to pressure gradients the wind flows from higher pressure regions to lower. This process is regular and unbalanced in between low and high speed. The kinetic energy of the wind pressure causes the wind to flow at seashore more than that of offshore. So maximum wind energy generating stations are located nearer to the seashore areas [5-7][39]. The Figure below depicts the detailed block diagram of a grid connected wind energy system. Here the model can be categorized into four componential areas; first is aerodynamic control which has wind flow, wind turbine blades and a hub which is interconnected with turbine blades. Second part is a mechanical assembled system having a gearbox and mechanical coupler with the shaft. Third one is electrical converter models having rotor side and grid side converter power electronics components [8][36]. The last one is the grid interface which is associated with the wind energy system under grid integrations. For standalone mode and island mode of operation the wind system is not connected to the grid. The wind flow causes the blade to rotate under low speed and high speed which develop mechanical motion inside the turbine and gearbox helps to fasten the speed of the rotor for a single rotation of blades [9][35]. The control schemes are also associated in each block for efficient output from the wind energy. The pitch angle controller controls the movement of the blades and activates itself under low speed and over speed of wind. The wind turbulence and wind flow makes the blades rotate and the mechanical system inside the hub helps to rotate the wind turbine [10][37]. This mechanical effect generates emf inside the synchronous generator that is used inside the system. The converter controls are categorized into two parts. First one is the rotor side controller and the second one is the grid side controller [11][38]. DFIGs can be very much useful for variable speed of operations. Simple PWM or Back to back converter models can be used to reduce the transients and can reduce the harmonics by a capacitor bank connected parallel. The grid interface connected directly to the grid side converter with transmission line parameters [12-14]. See Figure no. 1 shown below.

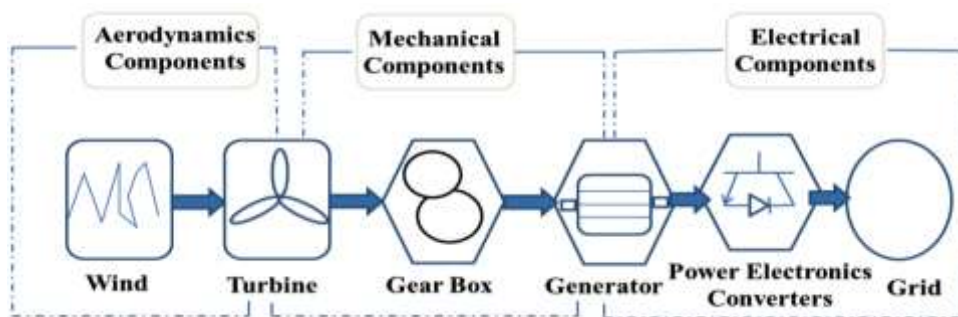


Figure 1: Designed Grid integrated Model of Wind Energy Conversion System

The maximum power of a wind turbine system using these type-III DFIGs can be increased by up to 30% compared to uncontrolled type-III DFIGs or partial controllers. Fixed speed and variable speed control techniques for wind energy generation are no longer effective. The fully controlled wind turbine systems are now widely deployed around the world. Permanent magnet based synchronous generators, also known as type-IV, are used to generate wind energy, however they are less useful than type-III due to their high cost [16]. These DFIGs are effective at controlling torque and speed. In DFIG-based systems, maintenance is required, whereas in Type-IV systems, maintenance is not required. The active and reactive power control can be done using this proposed model and studied in this research work [15][17][27].

#### 3.2 DFIG-Modified Type III Wind Turbine Systems

DFIGs are used in Type-III wind turbines to generate power at synchronous rotational speeds. The power smoothing of (P) active power and (Q) reactive power management utilizing the suggested technique discussed in the next section is displayed in Figure 2. This model includes a P control and Q control assembler that is directly connected to the control model in order to prevent errors that may occur during transient operations. The model's architecture is built on the dq reference frame, which works as a rotational frame for effective control action during transient [18][28][49-50].



### 3.4 Genetic Algorithm Optimization

The GA ratings may be accessed in MATLAB with the use of a complete DFIG model, which was used to validate the proposed GA technique. The wind speed in this model is kept constant at 10 m/s, and a distant failure on the 120kV system happens within the time (0.1 – 0.13 s), as shown in the Simulink diagrams. When comparing the results acquired using the standard PI controller in MATLAB to the results obtained using the GA approach to design the controller gains, the results obtained using the GA technique to create the controller gains show a significant increase in system dynamic performance. Under similar operating circumstances, GA is utilized to identify the optimum controller gains for the rotor and stator side converters. Figure 4 is shown below [2-5]. The modeling of wind turbine output power smoothing indices is demonstrated in Equations 11 and 12. The greater the output energy efficiency  $P_{eff}$ , the more efficient the Wind Turbine is, whereas the lower the  $P_{sm}$ , the less variation in the output of the Wind Turbine.

$$P_{eff} = \int_0^t |P_{wt}| dt \quad (11)$$

$$P_{sm} = \int_0^t |\Delta P_{wt}| dt \quad (12)$$

Here  $P_{wt}$  is Output power error which signifies the active power loss in the mathematical modeling and  $t$  is the simulation time.

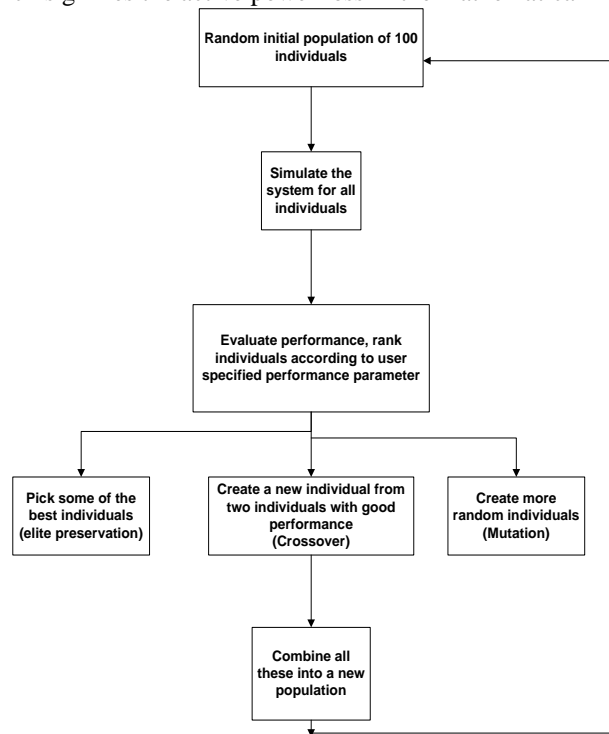


Fig. 4. Flow Chart for Genetic Algorithm Optimization Technique

The goal of the control approach is to have the measured levels of power absorbed into the grid to be equal to or close to the reference values. The reference active power is calculated using the wind speed and wind turbine parameters listed in the appendix, whereas the reactive power is calculated using the required reactive power converter correction. The reference reactive power is set to zero in this experiment. To keep the turbine speed at 1.09 pu, the control system employs a torque controller. There are four PI controllers in each of the GSC and RSC control loops, each of which has proportional and integral gain. The converter's behavior is determined by the control system. The grid side and rotor side converters' performance can be enhanced by adjusting these controllers to obtain optimal grid power without compromising the dynamic system's performance. The following objective function for RSC will be created in order to attain this aim:

$$F_1 = \int |i_{dr(ref)} - i_{dr}| + |i_{qr(ref)} - i_{qr}| + \{v_{dr}^2 + v_{qr}^2\}^{1/2} \quad (13)$$

$$F_2 = \int |i_{dg(ref)} - i_{dg}| + |i_{gr(ref)} - i_{gr}| + \{v_{dg}^2 + v_{qg}^2\}^{1/2} \quad (14)$$

Where  $i_{qg}$ ,  $i_{dg}$ ,  $i_{qr}$ ,  $i_{dr}$ ,  $v_{qg}$ ,  $v_{dg}$ ,  $v_{qr}$  and  $v_{dr}$  are the quadrature and direct components of both RSC and GSC currents and voltages.

Case 1: GA was solely used for RSC to improve the first goal function, which was linked to the rotor side converter.

Case 2: Using objective functions  $F_1$  and  $F_2$ , GA is applied to both RSC and GSC.

The end result In both cases, tables show the boundaries for controller gains and their optimal values as a result of using the GA solver. The findings are depicted in GA Simulink figures. The model's performance was compared to a full MATLAB Simulink model to demonstrate the investigation's validity [3][4]. In general, the figures show that employing the GA technique improves the dynamic responsiveness for each of the rotor and grid reference and measured currents, which are expressed by the first and

second terms in the objective functions that minimize the error between reference and measured currents. This correlates to improved dynamic performance for various DFIG variables, particularly the grid power curve, which moves closer to its reference value, achieving the main goal of the proposed GA method. The rotor voltage oscillations are considerably decreased, which contributes to improved DFIG safety and is critical to grid voltage stability. Because of the third term in the goal function that optimized the rotor voltage response, even in case 2 when the objective function is applied only for RSC, the dc link voltage oscillations clearly reduce and become closer to their reference value. In general, dc-link voltage fluctuations in both situations have no effect on the system's continuous operation, therefore increasing the DFIG dynamic performance [1][2][30-34].

### 3.5 Radial Basis Function Neural Network (RBFNN)

The RBFN network was chosen because of its ability to approximate a nonlinear input system to a linear output. Other NNs' training procedures are slower and less successful than the RBFNN's. It is useful for dynamic system modeling and control since it can approximate any continuous function with a certain level of precision. An input layer, a hidden layer, and an output layer make up the RBF NN. The RBF NN design is depicted in Figure 5. The RBF is found in the neurons of the buried layer, and its outputs are inversely proportional to the distance from the neuron's center. To produce their outputs, the output units use a weighted sum of the hidden unit's outputs.

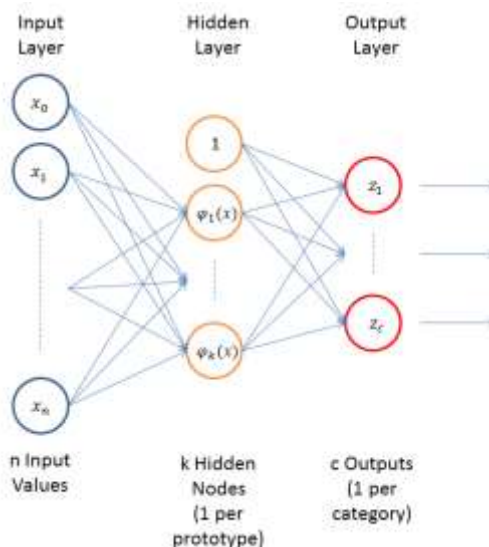


Fig. 5. RBF Network Structure

The multivariable NARX (nonlinear autoregressive exogenous model) model illustrated below following form may be used to represent the nonlinear system.

$$y(k) = f[y(k-1), \dots, y(k-ny), u(k-1-d), \dots, u(k-nu-d)] + e(k)$$

Here (\*) is the nonlinear function in vector form,  $e \in \mathcal{R}^p, u \in \mathcal{R}^m$ ,  $y$  are the noise vectors, process input and output respectively. Input member is denoted as  $m$  and output member denoted as  $p$ ,  $nu$  denotes input lag and  $ny$  denoted output lag,  $d$  is a the dead-time vector which represents delay in time for control variables of the nonlinearities.

Assume the RBF network model accurately represents the system; the model may then be expressed as follows:

$$\hat{y}(k) = f[\hat{y}(k-1), \dots, \hat{y}(k-ny), u(k-1-d), \dots, u(k-nu-d)] + e(k)$$

The input layer, hidden layer, and output layer are the three layers that make up the RBF NN. Each hidden node has a centre  $c_j$ , which is a cluster center defined by on the input vector  $x$ .

$$\|x(t) - c_j(t)\| \text{ with } x \text{ given as: } x(k) = [y(k-1), \dots, y(k-ny), u(k-1-d), \dots, u(k-nu-d)]$$

The hidden layer node's output is thus a nonlinear function of the Euclidean distance. The Gaussian function is used as the nonlinear function in this study.

$\varphi_i = e^{-\|x - c_i\|^2 / 2\sigma^2}, i = 1, \dots, nh$ ; here positive width scalar value is  $\sigma \in \mathcal{R}^{nh}$ , This is a distance scaling parameter that determines how far the unit will have a significant output in the input space. The input vector of the centre represented by  $c, x \in \mathcal{R}^{nh}$ .

The flowchart of RBFN optimization technique is shown below in figure no. 6.

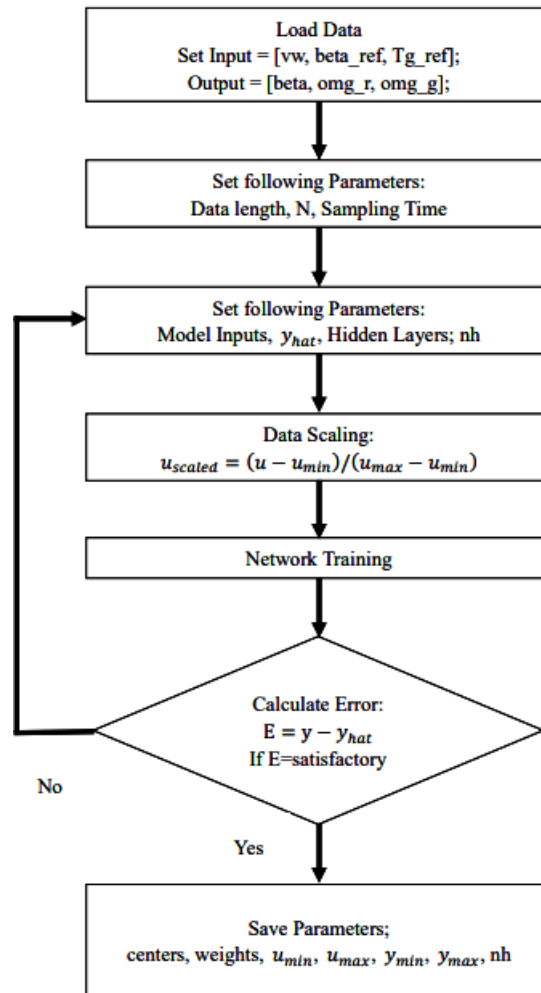


Fig. 6. Flow Chart for RBFN Technique

The network output is thus the total of all hidden nodes' weighted outputs plus bias. There are various sorts of functions that may be employed in addition to the Gaussian basis function, such as thin plate spine. The Gaussian basis function, on the other hand, was chosen because it is selective and responds to inputs that fall inside the region. Gaussian functions may be used to describe a wide range of mathematical, scientific, and engineering processes. It may be used to accurately estimate a large number of nonlinear continuous functions specified on a small set. [1] [6]

In this study, network centers are clustered using the K-means approach, with the goal of reducing the total squared distance between each input data point and the centre of the data group to which it belongs. The widths of the Gaussian functions are chosen using the p-nearest center technique, which ensures that any input data is suitably sampled by a few near centers. Because it is a numerically robust approach, the recursive least squares (RLS) technique is employed to train the weights between the hidden layer and the output.

The centers are determined using the K-means clustering technique, which aims to reduce the sum squared distances between each input data point and its nearest center, ensuring that the data is properly covered by the activation functions  $\Phi_j(t)$ . The following is how the K-means clustering algorithm works:

1. Take the cluster centers  $q$  as initial cluster centers  $c_1(1), c_2(1), \dots, c_q$
  2. Distribute the sample at the  $t$  time step ( $x$ ) into  $S_j(t)$  among the  $q$  cluster domains.  $S_j(t)$  signifies the set of samples that make up the cluster  $c_j(t)$   $x \in S_j(t)$  if  $\|x(t) - c_j(t)\| < \|x(t) - c_i(t)\|$  where,  $j = 1, 2, \dots, q$  and  $i = 1, 2, \dots, j-1, j+1, q$ .
  3. The cluster centers should be updated.  $c_j(t+1) = \frac{1}{N_j} \sum S_j(t)$
- here,  $N_j$  is the total number of components in  $S_j(t)$ .
4. Steps 2 and 3 should be repeated until  $c_j(t+1) = c_j(t)$ .

Each unit's RBF NN width  $\sigma$  is calculated using the p-nearest neighbor technique. The rule is that each node's excitation should overlap with some other nodes, generally the nearest, in order to provide a smooth surface interpolation between nodes. To do

this, each hidden node must significantly activate at least one other hidden node. As a result, the breadth is chosen to be bigger than the distance from the nearest unit center.

$$\sigma_i = \left[ \frac{1}{p} \sum_{j=1}^p |c_i - c_j|^2 \right]^{1/2}$$

Here  $i = 1, 2, \dots, q$ , and  $c_j$  is the  $p$ -nearest neighbors of  $c_i$ . A nonlinear function approximation,  $p$  is determined by the problem and must be validated.

This Recursive Least Squares (RLS) algorithm is a recursive version of the Least Squares (LS) method. It recalculates the parameter matrix  $W$  for each new sample. The RLS method works by adding some correction information to the prior parameter estimate  $W(t-1)$  at time instant  $t-1$  to produce the new parameter estimate  $W(t)$  at discrete time steps  $t$ . It's utilized to calculate the RBF network weights  $W$ , which are as follows:

$$Y_p(t) = Y_c(t) - (t-1)h(t)$$

$$g_z(t) = P_z(t-1)h(t) \mu + h^T(t)P_z(t-1)h(t) \quad P_z(t) = \mu^{-1} [P_z(t-1) - g_z(t)h^T(t)P_z(t-1)] \quad W(t) = W(t-1) + g_z(t)Y_p(t)$$

The RBF network weights represented as  $W$  and activation function outputs are represented by  $h$ . The output process represented as  $Y_c$  in vector form and prediction error value presented here as  $Y_p$ . This is the difference between the predicted and measured output value. The intermediate terms are presented as  $P_z$  and  $g_z$ . The forgetting factor is a number that ranges from 0 to 1 and is set to 1 during off-line training. With the change in the activation function output  $h$ , the parameters  $g_z$ ,  $w$ , and  $P_z$  are changed in order for each sample.

### 3.6 RBFN Wind Turbine Model

All raw data samples were standardized into the range of [0, 1] after data collection and before the training and testing method to improve the NN's accuracy and reduce error. The following equations were used to create the linear scale:

$$u_{scale}(k) = \frac{u(k) - u_{min}}{u_{max} - u_{min}} \quad y_{scale}(k) = \frac{y(k) - y_{min}}{y_{max} - y_{min}}$$

In the above equation  $u_{min}$  represent minimum input data sets,  $u_{max}$  represents maximum input data sets and  $y_{max}$  represents the output data set is maximum value,  $u_{scale}$  represents scaled input value and  $y_{scale}$  represents the output scaled value of the wind model.

This mean absolute error (MAE) is employed instead of the mean square error (MSE) because of MAE may precisely measure the error's amplitude, meanwhile the MSE only indicates the squared error only rather not just the error itself. The MAS is written as follows:

$$e_{MAE} = \frac{1}{N} \sum_{t=1}^N |f(t) - y(t)| = \frac{1}{N} \sum_{t=1}^N |e(t)|$$

The MAE is a calculation that takes the absolute error and averages of it represent as  $e(t) = f(t) - y(t)$ . Here,  $f(t)$  indicates the NN model's prediction value, while  $y(t)$  reflects the output of the wind turbine system.

Hence the next design step is to the next step is to calculate the RBF model's input variable with respect to design parameters. A wind turbine system designed according to Type-III WTs consists of three input variables. First one is speed of the wind represented as ( $v_w$ ), second one is blade pitch angle ( $\beta_{ref}$ ) (reference) and the third variable is electromagnetic torque ( $T_g$ ) developed during operation. The output variables taken here as blade pitch angle ( $\beta$ ) which control the wind speed and active when wind speed varies. The second output variable is rotor speed ( $\Omega_r$ ) which calculated under steady state and transient state. The third output parameter is generator speed ( $\Omega_g$ ) which coupled with the rotor as sliding surface. The trial and error method employed to design the RBF model for a wind turbine system using DFIG. Errors during modeling taken care using control parameters. In the model training, many time delays and ordering parameters of these variables were explored and the one with the smallest training error was taken into consideration. The formula for the WT design is as follows:

$$\hat{y}(k) = f[\hat{y}(k-1), \hat{y}(k-2), \hat{y}(k-3), u(k-1), u(k-2), u(k-3)] + e(k)$$

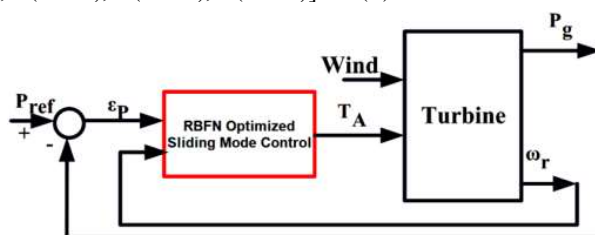


Fig. 7. RBFN Optimized SMC in wind turbine

In the above figure no. 7, the RBFN model is implemented which operated by input parameters as stated above and the power error also taken into consideration which produced by the rotor. For smooth design 20 parameters are taken here as input variable and three major output parameters are taken as nodes of algorithm. The Gaussian functions for the 12 hidden nodes of the model use the same width as follows. 12 hidden nodes are taken with respect to the input variables. K mean clustering technique employed to determine the centers of the ANN and p-nearest neighbor's algorithm used to calculate width  $\sigma$  of the model. This method was trained using the RLS algorithm that was created, using the following starting values:  $\mu = 0.998$ ,  $(0) = 1.02 \times 10^{-6} \times U(nh \times 3)$ ,  $P(0) = 1.0 \times 110 \times I(nh)$ , The number of hidden layers is given by  $nh$ . Where  $U$  is the matrices with all elements having the unity value,  $\mu$  represents forgetting factor and  $I$  represents the identity matrix of the model equation. [51-55]

### 3.7 Sliding Mode Controller Optimization

Internal inaccuracies, nonlinearity in parametric fluctuations, and anomalies that were not accounted for in the modeling are all well-known features of this modern technique. The SMC approach can be utilized to improve the rotor's stability when the wind speed changes. [40-44] On the sliding surface of limitations of control gains and laws, non linearity owing to changeable wind speed in the rotor side of the DFIG can be removed. [57] This procedure enhances the robustness of the sliding surface of the rotor block. Figure 8 shown below illustrates the basic phasor representation of sliding surface for the desired speed and the errors due to the speed variations. The rotor torque can be improved by minimizing the error and rotor power can be increased by this phenomena. There are three constraints designs are presented to implement the proposed control technique to the wind turbine system. [10][45-48][56]

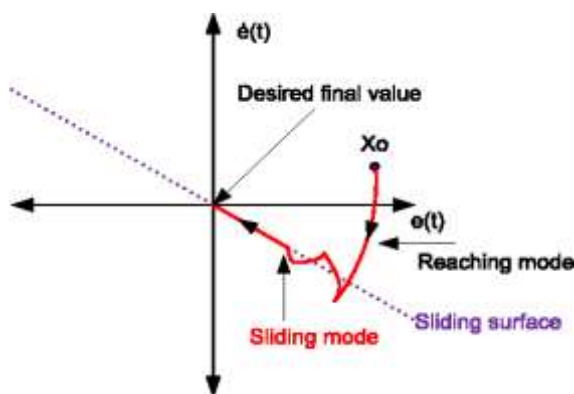


Fig. 8. Sliding Mode Control Phasor [8]

For increasing robustness sliding mode control technique can be designed in three stages. They are:

#### a. Selection of sliding surfaces

The surface of sliding is taken as scalar function to control the slip of the rotor. It is represented as follows:

$$s(x) = \left(\frac{d}{dt} + \lambda\right)^{r-1} e(x) \quad (11)$$

where,  $\lambda$  is a positive wind constant,  $r$  is the relative degree of the system, and the error between the variable and its reference is denoted by  $e(x)$ . For the command of the power taking  $r=1$ ; we get:

$$s(x) = e(x) \quad (12)$$

The active power is proportional to the rotor axis current  $q$ , whereas the reactive power is directly proportional to the rotor axis current  $d$ .

$$s(P) = e(P) = I_{rq\_ref} - I_{rq} \quad (13)$$

$$s(Q) = e(Q) = I_{rd\_ref} - I_{rd} \quad (14)$$

Hence we get:

$$s'(p) = -\frac{L_s}{V_s L_m} p_{s\_ref} \frac{1}{L_r \sigma} (V_{rq} - R_r I_{rq} - \omega_r L_r \sigma L_{rd} - \omega_r \frac{L_m}{L_s L_s}) \quad (15)$$

$$s'(Q) = -\frac{V_s}{\omega_s L_m} p_{s\_ref} \frac{1}{L_r \sigma} (V_{rd} - R_r I_{rd} - \frac{L_m}{L} \frac{d\psi_s}{dt} + \omega_r L_n \sigma I_{rq}) \quad (16)$$

#### b. Convergence Requirements (Conditions)

Both sliding surfaces must be taken zero in order to compel the chosen variables to converge with their reference values.

$$s'(P) = 0 \Rightarrow s(P) = \frac{d}{dt} (I_{rq\_ref} - I_{rq}) = 0 \quad (17)$$

$$\dot{s}(Q) = 0s(Q) = \frac{d}{dt} (I_{rd\_ref} - I_{rd}) = 0 \quad (18)$$

### c. Design of a control laws

Considering the following commands for the design:

$$\dot{s}(P) = -\text{sgn}(s(P)) \quad (19)$$

$$\dot{s}(Q) = -\text{sgn}(s(Q)) \quad (20)$$

Combining the Equation (19) with Equation (20) and designing the whole control laws, the combined sliding control system presented as follows:

$$\frac{L_s}{v_s L_m} p_{s\_ref} \frac{1}{L_r \sigma} (V_{rq} - R_r I_{rq} - \omega_r L_r \sigma L_{rd} - \omega_r \frac{L_m}{L_s L_s}) = \text{sgn}s(P) \quad (21)$$

$$\frac{1}{L_r \sigma} (V_{rd} - R_r I_{rd} - \frac{L_m}{L} \frac{d\psi_s}{dt} + \omega_r L_n \sigma I_{rq}) = \text{sgn}s(Q) \quad (22)$$

Using the above global sliding control equations rotor voltage can be written as follows:

$$V_{rq} = R_r I_{rq} + \omega_r L_r \sigma L_{rd} - g_{L_s}^{L_m V_s} + \sigma L_r L_{rq\_ref} \quad (23)$$

$$V_{rq_0} = R_r I_{rd} + \omega_r L_r \sigma L_{rq} \quad (24)$$

The algorithm of control is defined by the relation:

$$V_{rq} = V_{rq\_Eq} + V_{rq\_attr} \quad (25)$$

$$V_{rd} = V_{rd\_Eq} + V_{rd\_attr} \quad (26)$$

$$V_{rq\_attr} = -V_1 (\text{sat}(\dot{s}(P))) \quad (27)$$

$$V_{rd\_attr} = -V_2 (\text{sat}(\dot{s}(Q))) \quad (28)$$

Combining all control law equations we get:

$$V_{rq\_attr} = L_r (\text{sgn}(e(P))) \quad (29)$$

$$V_{rd\_attr} = L_r (\text{sgn}(e(Q))) \quad (30)$$

$$V_{rq\_Eq} = R_r I_{rq} + \omega_r L_r \sigma L_{rd} - g_{L_s}^{L_m V_s} + \sigma L_r L_{rq\_ref} \quad (31)$$

$$V_{rd\_Eq} = R_r I_{rd} + \omega_r L_r \sigma L_{rq} \quad (32)$$

The global sliding mode control equations helps in generalizing the rotor side and grid side converter parameters. [58-60]

## 4. SIMULINK RESULTS

Here voltage and electromagnetic torque is carried out by sliding mode controller to remove nonlinearities. See figure no. 8 and 9.

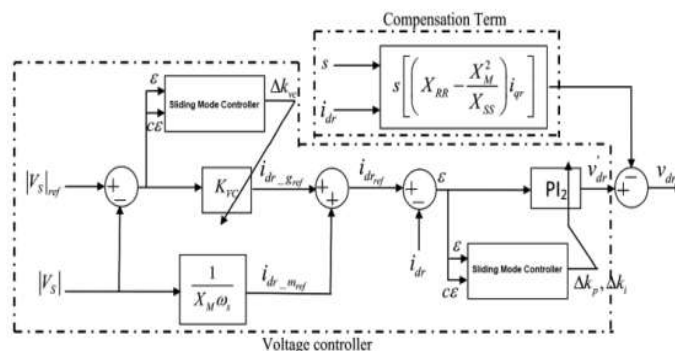


Fig. 9.SMC in Voltage Control

The above figure no. 9 illustrates the voltage control strategy using the sliding mode controller on the errors due to PI-FLC gain values. The reference and the actual voltage in terms of compensation can be modified according the feedbacks. The nonlinearities in voltage due to wind speed can be controlled by gain values of the proposed controller technique.

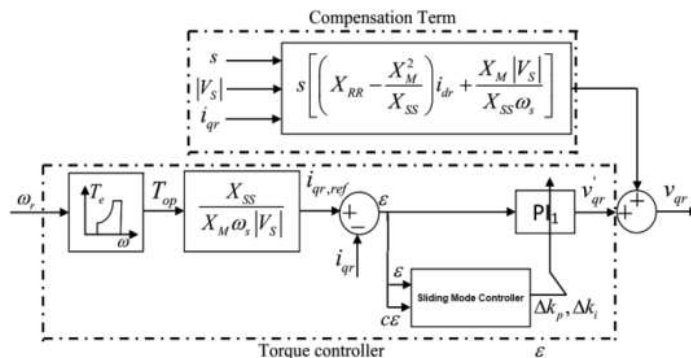


Fig. 10.SMC in Torque Control

The figure no. 10 illustrates the torque control strategy using the sliding mode controller on the errors due to PI-FLC gain values. The reference and the actual torque values of sliding surface in terms of compensation can be modified according the feedbacks. The nonlinearities in torque can control the rotor power under rapid wind speed variations. This can be controlled by gain values of the proposed controller technique by controlling the stator voltage, rotor current and slip associated with the rotor surface. The comparative results are shown below which clarifies that the power smoothing can be done by reducing the nonlinearities. From above simulation the results are shown below. Figure no. 11 illustrates the Comparison on Generated Power, Figure 12 illustrates Comparison on Output Power (Smoothing in Reactive power Compensation) and Figure 13 illustrates the Maximum Energy Comparison with respect to Active Power Loss Function

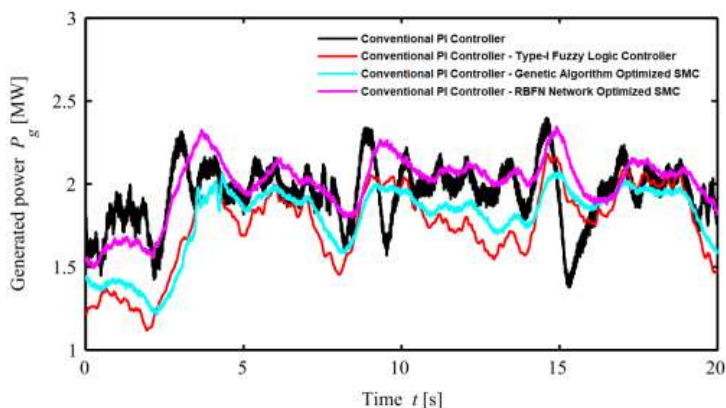


Fig. 11. Comparison on Generated Power

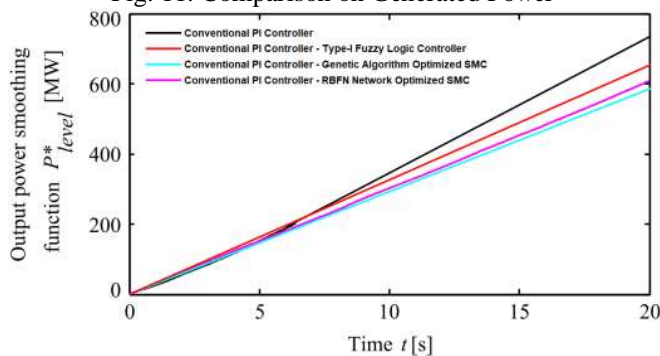


Fig. 12. Comparison on Output Power (Smoothing in Reactive power Compensation)

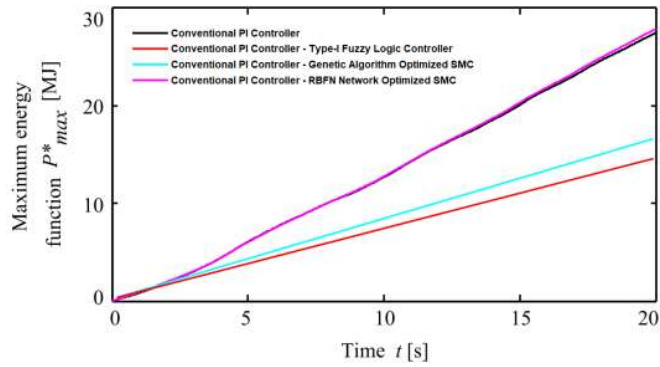


Fig. 13. Maximum Energy Comparison with respect to Active Power Loss Function

The comparative results of cut in speed, nominal speed and cut out speed are illustrated in figure no. 14 to figure no. 28 respectively.

**a. Results for wind speed 4m/s (Cut in Speed)**

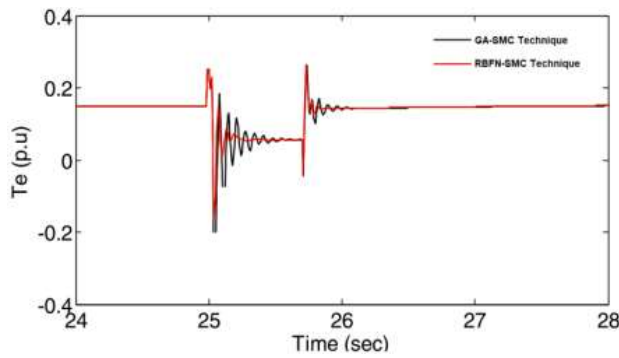


Fig. 14. Nonlinearity in Torque

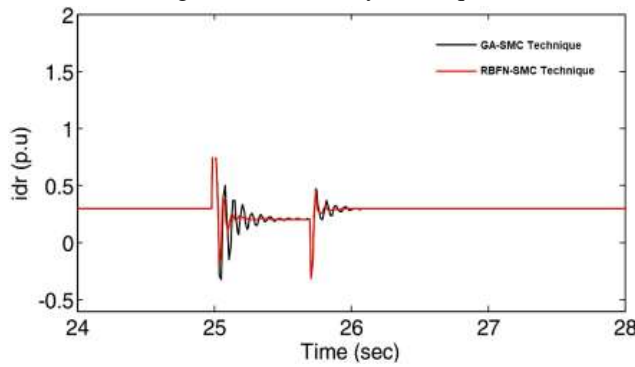


Fig. 15. Nonlinearity in d axis rotor current

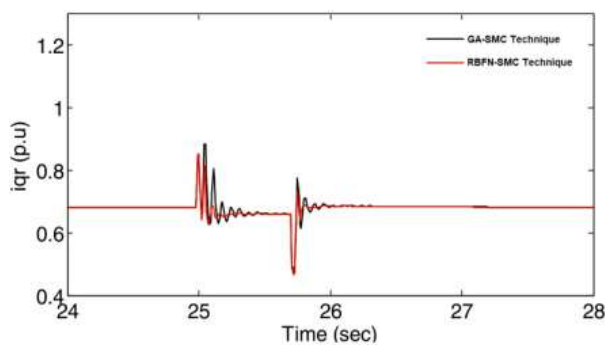


Fig. 16. Nonlinearity in q axis rotor current

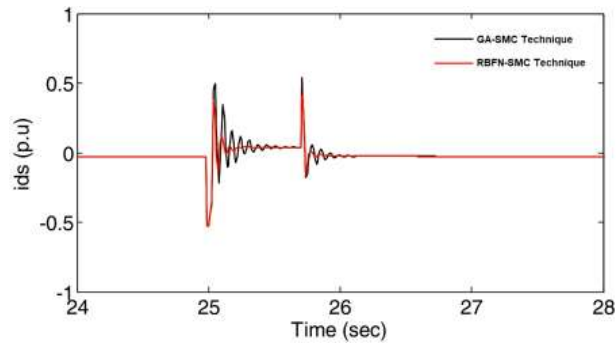


Fig. 17. Nonlinearity in d axis stator current

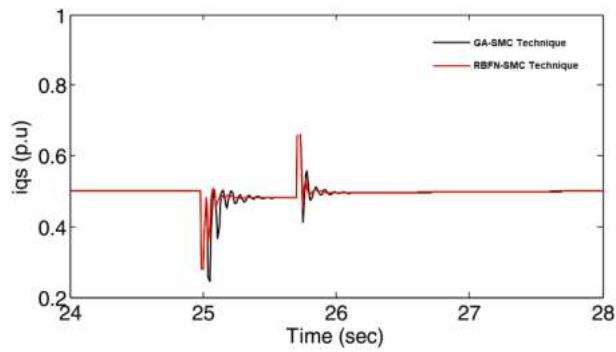


Fig. 18. Nonlinearity in q axis stator current

**b. Results for wind speed 8m/s (Nominal Speed)**

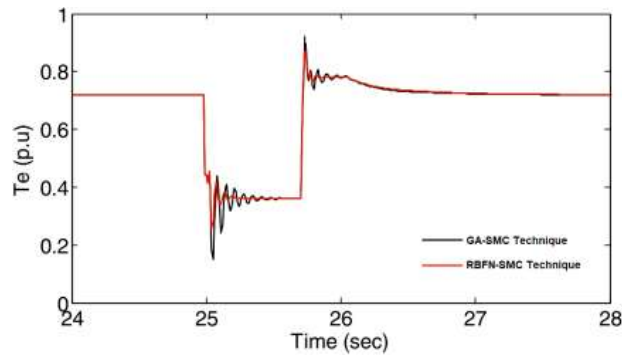


Fig. 19. Nonlinearity in Torque

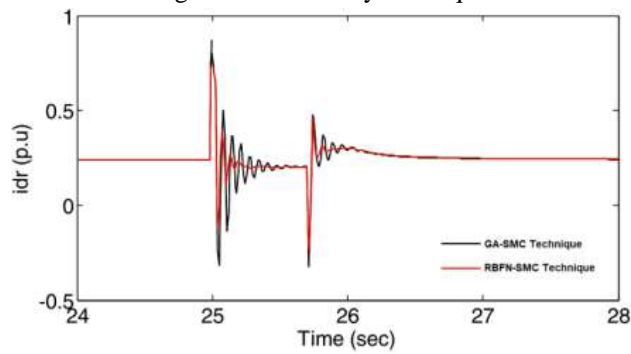


Fig. 20. Nonlinearity in d axis rotor current

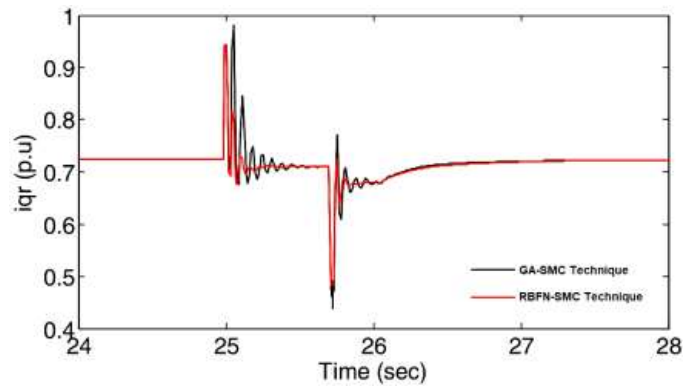


Fig. 21. Nonlinearity in q axis rotor current

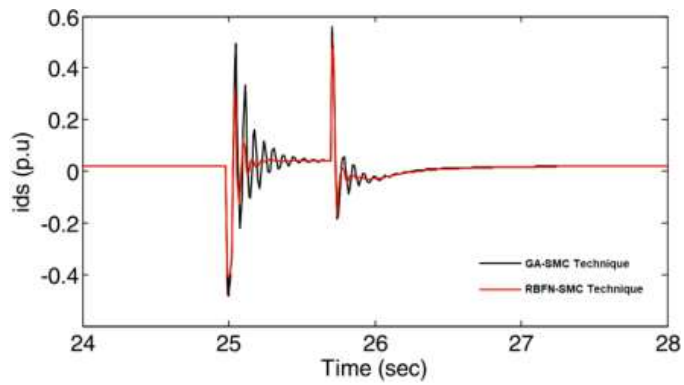


Fig. 22. Nonlinearity in d axis stator current

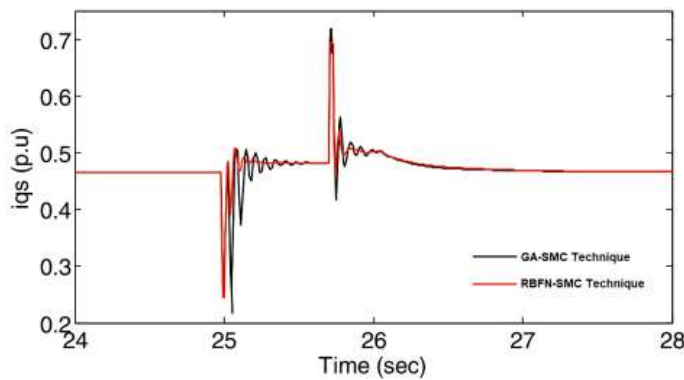


Fig. 23. Nonlinearity in q axis stator current

**c. Results for wind speed 12m/s (Cut out Speed)**

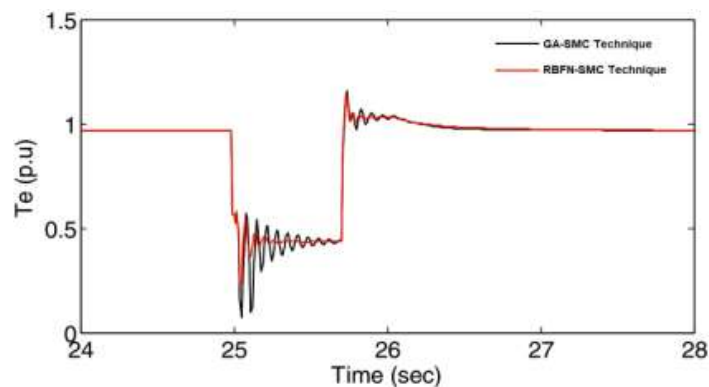


Fig. 24. Nonlinearity in Torque

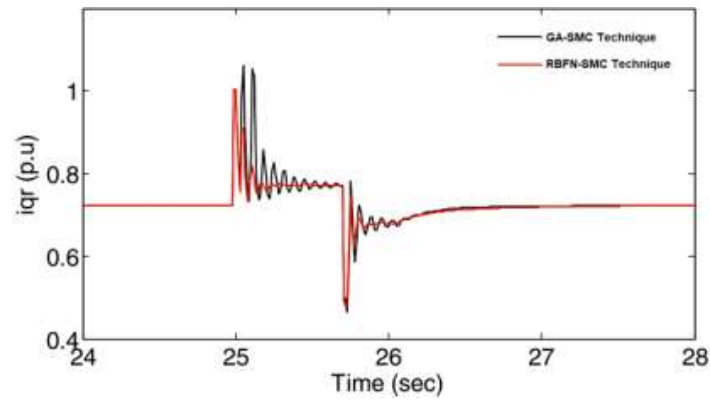


Fig. 25. Nonlinearity in d axis rotor current

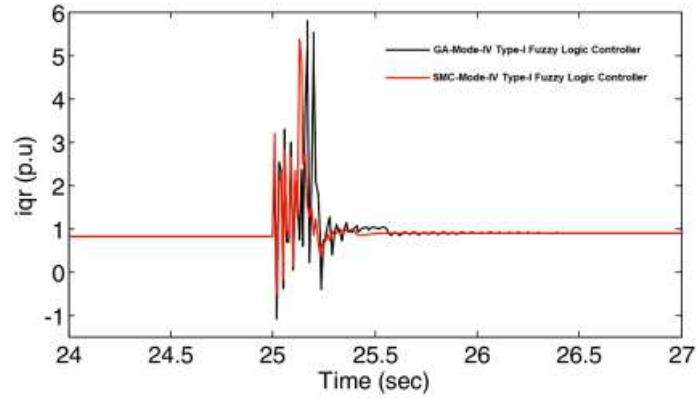


Fig. 26. Nonlinearity in q axis rotor current

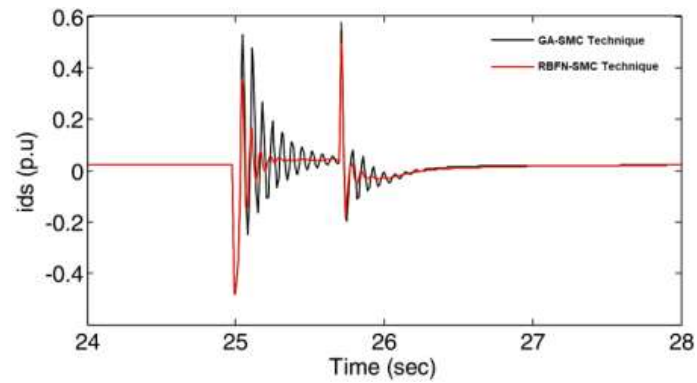


Fig. 27. Nonlinearity in d axis stator current

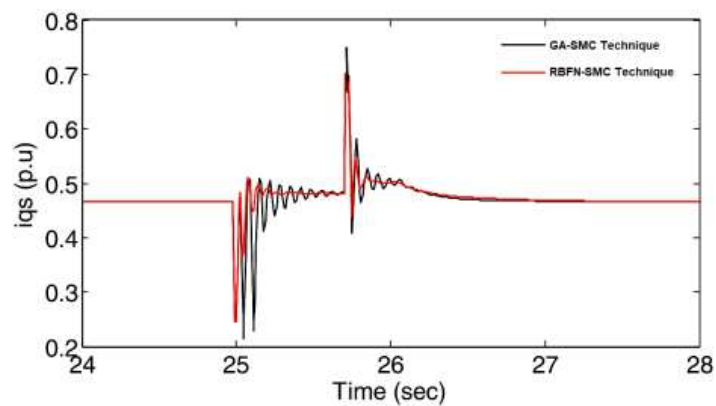


Fig. 28. Nonlinearity in q axis stator current

#### d. Torque and Power Comparison with Sliding Mode Controller

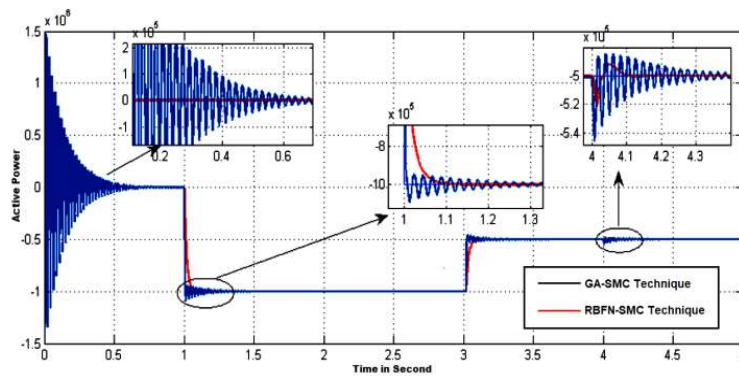


Fig. 29. Active Power in Watt vs Time in Second

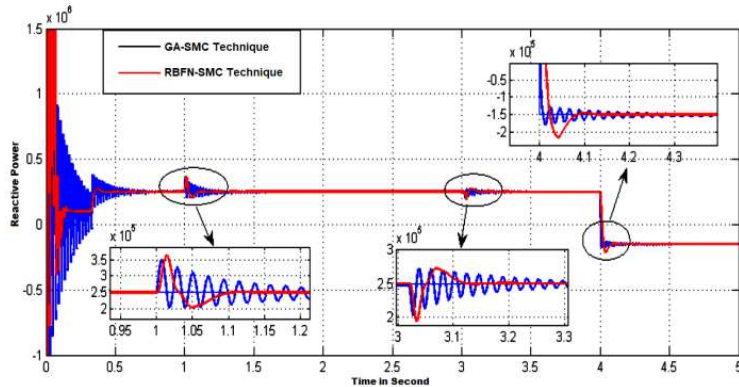


Fig. 30. Reactive Power in Watt vs Time in Second

Figure 29 depicts the active power variation with respect to time, while figure 30 depicts the reactive power variation with respect to time, based on the preceding results. Based on the foregoing findings, it can be inferred that nonlinearities can be reduced by employing a sliding mode controller in conjunction with the recommended methodologies.

#### e. Stability Analysis using Bode Plot and Nyquist Plot

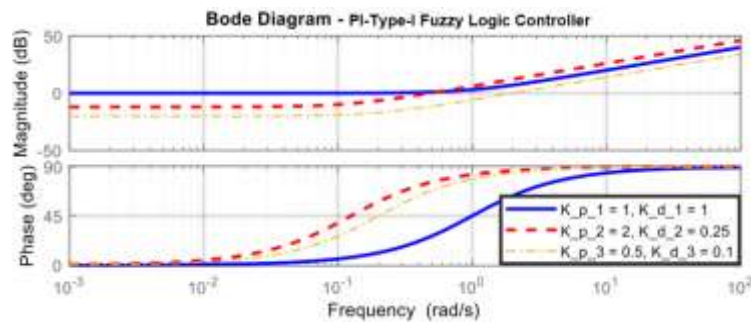


Fig. 31. Bode Plot Stability Analysis using PI-Type-I FLC

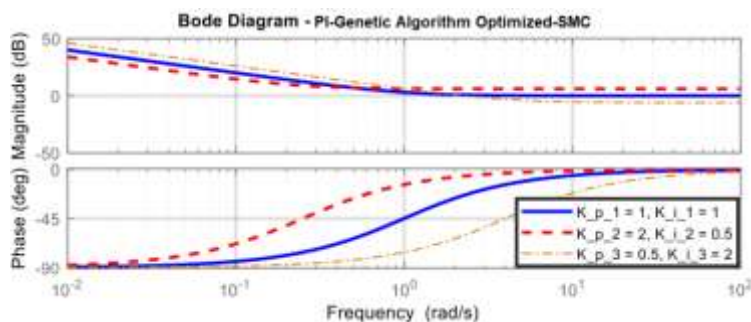


Fig. 32. Bode Plot Stability Analysis using PI-GA-SMC

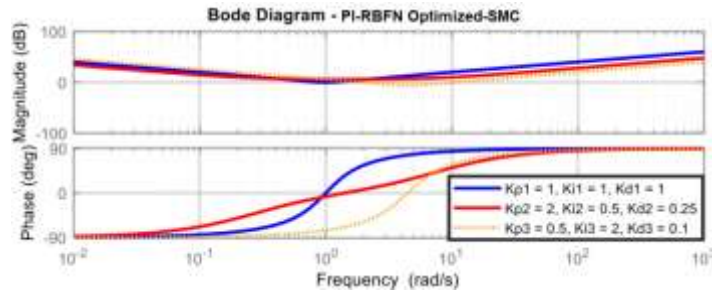


Fig. 33. Bode Plot Stability Analysis using PI-RBFN-SMC

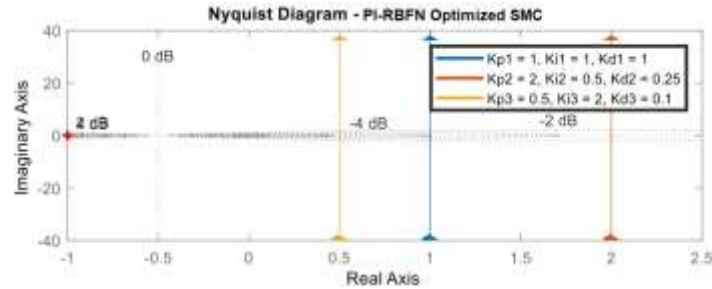


Fig. 34. Nyquist Plot Stability Analysis using PI-Type-I FLC

From the Bode plots and Nyquist plots in Figures 31 to 34, it can be seen that the PI-RBFN-SMC (Proportional-Integral-Radial Basis Function Network-Sliding Mode Controller) technique exhibits greater steady state and transient stability under changes in wind energy system characteristics than the GA-based SMC technique.

### 5. Discussion

The nonlinearities due to parameters like wind speed, mechanical torque of the rotor, converter harmonics and reactive power taken into consideration to study and validate the model. The simulink results are presented in below in the form of tabulation. Figure 35 shown below illustrates the complete working model for the approach. Here the three control levels are introduced where the proposed techniques are implemented.

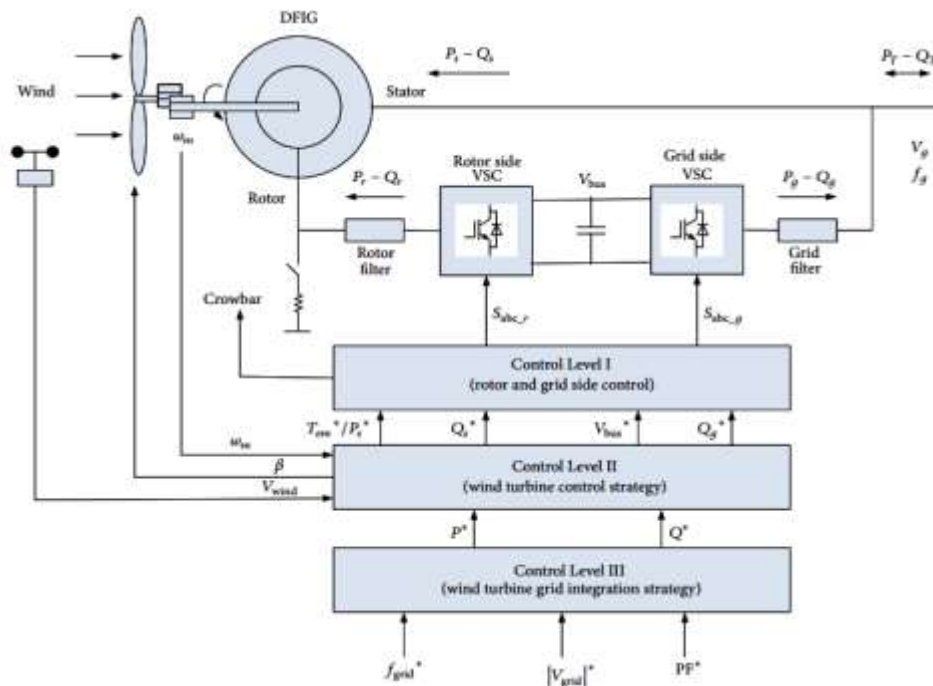


Fig. 35 Complete working model for WECS

Table 1 Comparison of Wind Turbine Parameters using Various Controllers

Controller	Conventional PI Controller	PI-Fuzzy Logic Controller	PI-Mode-IV-Fuzzy Logic Controller	PI-M4T1FLC-GA	PI-M4T1FLC-GA-SMC	PI-M4T1FLC-RBFN-SMC
Wind Power Coefficient	-0.447	-0.352	-0.375	-0.013	-0.015	-0.0151
Wind Torque	-0.290	-0.280	-0.271	+0.049	+0.056	+0.057
Wind Power Error	-0.286	-0.275	-0.270	+0.052	+0.058	+0.060
Efficiency ( $P_{eff}$ )	-70.5	-79.5	-80.5	-81.6	+0.09	+0.095
$P_{sm}$	+70.20	+79.25	+80.25	+80.26	+0.05	+0.052

The comparison table 1 for various wind energy characteristics shows that the proposed technique is effective in reducing nonlinearities and increasing rotor torque and power. Under abrupt wind speed variations, the wind efficiency of a modified Type-III wind turbine system rose by up to 95% employing the RBFN-sliding mode control technology.

Table 2 Comparison of Wind Turbine Tuning Parameters using Various Controllers

Controller	Conventional PI Controller	PI-Fuzzy Logic Controller	PI-Mode-IV-Fuzzy Logic Controller	PI-M4T1FLC-GA	PI-M4T1FLC-GA-SMC	PI-M4T1FLC-RBFN-SMC
Maximum Overshoot (%)	10.542	7.125	5.121	4.845	3.712	2.885
Peak Time (Sec)	0.016	0.025	0.038	0.052	0.075	0.164
% of Error	0.335	0.442	0.560	0.630	0.775	2.905
ISE	9.5420	8.3035	8.3235	8.0012	6.7505	6.711
ITAE	75.5567	70.7890	69.1005	63.7652	63.8086	62.7660

The generally used performance criteria in stability analysis includes Integral time absolute error(ITAE), Integral square error (ISE), Integral time square error(ITSE) and Integral absolute error (IAE).

Table 3 Comparison Cut in Speed (4m/s): Power Losses for various Voltages under transients (Per Unit Calculation)

Controller Software	Type- I FLC PID Controller	Type- I FLC Mode-IV Controller	GA-Type- I FLC Mode-IV Controller	PI-GA-SMC Controller	PI-RBFN-SMC Controller
Active Power	1.25	1.26	1.25	1.26	1.265
Reactive Power	0.85	0.91	1.01	1.13	1.154
Active Power Loss	0.40	0.35	0.24	0.13	0.111
Settling Time	12.077 msec	11.35msec	10.75 msec	10.70 msec	10.69 msec

Table 4 Comparison Nominal Speed (8m/s): Power Losses for various Voltages under transients (Per Unit Calculation)

Controller Software	Type- I FLC PID Controller	Type- I FLC Mode-IV Controller	GA-Type- I FLC Mode-IV Controller	PI-GA-SMC Controller	PI-RBFN-SMC Controller
Active Power	1.25	1.26	1.25	1.27	1.275
Reactive Power	0.89	1.05	1.10	1.14	1.156
Active Power Loss	0.36	0.21	0.15	0.13	0.119
Settling Time	12.075 msec	11.86 msec	10.58 msec	10.55 msec	10.545msec

Table 5 Comparison cut out Speed (12m/s): Power Losses for various Voltages under transients (Per Unit Calculation)

Controller Software	Type- I FLC PID Controller	Type- I FLC Mode-IV Controller	GA-Type- I FLC Mode-IV Controller	PI-GA-SMC Controller	PI-RBFN-SMC Controller
Active Power	1.25	1.26	1.25	1.29	1.31
Reactive Power	0.89	1.05	1.10	1.148	1.163
Active Power Loss	0.36	0.21	0.15	0.142	0.147
Settling Time	12.075msec	11.86msec	10.58 msec	10.549msec	10.538msec

Table 2 illustrate comparison of wind turbine tuning parameters using various controllers, Table 3 illustrate Comparison Cut in Speed (4m/s): Power Losses for various Voltages under transients (Per Unit Calculation), Table 4 illustrate Comparison Nominal Speed (8m/s): Power Losses for various Voltages under transients (Per Unit Calculation) and Table 5 illustrate Comparison Cut Out Speed (12m/s): Power Losses for various Voltages under transients (Per Unit Calculation). From the above Simulink results it is found that the proposed controller can be suitable for the power smoothing under transients.

## 6. CONCLUSION

Electricity production from wind energy system is the most economical and freely available source of generation for the modern power system, with no harmful emissions. As a result, by upgrading this renewable source with innovative technology, we may increase power production while retaining the stability of our contemporary power grid. This suggested control method, when combined with a sliding mode controller, significantly improves power efficiency. Obliquely, limiting active power losses due to wind speed fluctuations is incredibly efficient. Using RBFN artificial neural network optimization, it is possible to reduce power loss by 85-95 percent of its generation. Wind speed fluctuations create rotor torque nonlinearities, which can be successfully minimised and torque improved up to 40% of rated torque by reducing nonlinearities caused by wind speed fluctuations. With SMC-RBFN, rotor power can be increased by 50-60% of rated power. The steady state was reached 25-35 percent faster with SMC-RBFN than with SMC-GA, and the settling time under transient conditions was reduced by 20% compared to conventional controllers. As a result, this article will aid researchers in developing alternative evolutionary algorithms that use SMC and ANN to eliminate nonlinearities and enhance both steady state and transient power system stability.

## References

- [1] A. H. Sule, A. S. Mokhtar, J. J. Bin Jamian, U. U. Sheikh and A. Khidrani, "Grey Wolf Optimizer Tuned PI Controller for Enhancing Output Parameters of Fixed Speed Wind Turbine," 2020 IEEE International Conference on Automatic Control and Intelligent Systems (I2CACIS), 2020, pp. 118-122, doi: 10.1109/I2CACIS49202.2020.9140171.
- [2] Andrade, I.; Pena, R.; Blasco-Gimenez, R.; Riedemann, J.; Jara, W.; Pesce, C. An Active/Reactive Power Control Strategy for Renewable Generation Systems. Electronics 2021.
- [3] Ardjal A, Mansouri R, Bettayeb M. Fractional sliding mode control of wind turbine for maximum power point tracking. Transactions of the Institute of Measurement and Control. 2019;41(2): 447-457.
- [4] M. Malmir, H. Momeni and A. Ramezani, "Controlling Megawatt Class WECS by ANFIS Network Trained with Modified Genetic Algorithm," 2019 27th Iranian Conference on Electrical Engineering (ICEE), 2019, pp. 939-943, doi: 10.1109/IranianCEE.2019.8786748.
- [5] M. M. A. Rahman and A. H. M. A. Rahim, "Design and Testing of an MPPT Algorithm Using an Intelligent RBF Neural Network and Optimum Relation Based Strategy," 2020 IEEE Region 10 Symposium (TENSymp), 2020.
- [6] Y. Belkacem, S. Drid, A. Makouf, L. Chrifi-Alaoui and M. Ouriagli, "Fuzzy Controllers for a high performance of the Doubly Fed Induction Generator based on Wind Turbine in variable speed," 2019 International Conference on Intelligent Systems and Advanced Computing Sciences (ISACS), Taza, Morocco, 2019, pp. 1-7.
- [7] J. Gu, B. Meng, H. Ren, J. Zhu, Z. Chen and H. Li, "Design of the Wind Turbine Simulation System Based on Fuzzy Control," 2019 6th International Conference on Systems and Informatics (ICSAI), Shanghai, China, 2019, pp. 268-273.
- [8] M. Zerouali, M. Boutouba, A. E. Ougli and B. Tidhaf, "Control of variable speed wind energy conversion systems by fuzzy logic and conventional P&O," 2019 International Conference on Intelligent Systems and Advanced Computing Sciences (ISACS), Taza, Morocco, 2019, pp. 1-5.
- [9] M. Ferrari, M. Orendorff, T. Smith and M. A. Buckner, "Open-Code, Real-Time Emulation Testbed Of Grid-Connected Type-3 Wind Turbine System With Hardware Validation," 2019 IEEE Applied Power Electronics Conference and Exposition (APEC), Anaheim, CA, USA, 2019, pp. 66-70.

- [10] I. Poultangari, R. Shahnazi and M. Sheikhan, "RBF neural network based PI pitch controller for a class of 5-MW wind turbines using particle swarm optimization algorithm", *ISA Trans*, vol. 51, no. 5, pp. 641-648, 2012.
- [11] S. Soued, M. A. Ebrahim, H. S. Ramadan and M. Becherif, "Optimal blade pitch control for enhancing the dynamic performance of wind power plants via metaheuristic optimisers", *IET Electr. Power Appl*, vol. 11, no. 8, pp. 1432-1440, 2017.
- [12] M. Q. Duong, F. Grimaccia, S. Leva, M. Mussetta, K. H. Le and L. District, "Improving Transient Stability in a Grid-Connected Squirrel-Cage Induction Generator Wind Turbine System Using a Fuzzy Logic Controller", *energies*, vol. 8, pp. 6328-6349, 2015.
- [13] B. Zahra, H. Salhi and A. Mellit, "Wind turbine performance enhancement by control of pitch angle using PID controller and particle swarm optimization", *2017 5th International Conference on Electrical Engineering - Boumerdes ICEE-B 2017*, pp. 1-5, 2017.
- [14] Z. Civelek, "Optimization of fuzzy logic (Takagi-Sugeno) blade pitch angle controller in wind turbines by genetic algorithm", *Eng. Sci. Technol. an Int. J.*, vol. 23, no. 1, pp. 1-9, 2019.
- [15] S. Soued, M. A. Ebrahim, H. S. Ramadan and M. Becherif, "Optimal blade pitch control for enhancing the dynamic performance of wind power plants via metaheuristic optimisers", *IET Electr. Power Appl*, vol. 11, no. 8, pp. 1432-1440, 2017.
- [16] M. Q. Duong, F. Grimaccia, S. Leva, M. Mussetta, K. H. Le and L. District, "Improving Transient Stability in a Grid-Connected Squirrel-Cage Induction Generator Wind Turbine System Using a Fuzzy Logic Controller", *energies*, vol. 8, pp. 6328-6349, 2015.
- [17] Boukhezzar, B, Siguerdidjane, H, Nonlinear control of a variable-speed wind turbine using a two-mass model. *IEEE Transactions on Energy Conversion*, 2011, 26(1): 149–162.
- [18] Wang, Z, Yuan, J, Pan, Y (2017) Adaptive second-order sliding mode control: A unified method. *Transactions of the Institute of Measurement and Control*. Epub online ahead of print 3April2017. DOI: 10.1177/0142331217694683.
- [19] Yang, B, Jiang, L, Wang, L. (2016) Nonlinear maximum power point tracking control and modal analysis of DFIG based wind turbine. *International Journal of Electrical Power & Energy Systems* 74: 429–436.
- [20] J. W. Choi, S. Y. Heo and M. K. Kim, "Hybrid operation strategy of wind energy storage system for power grid frequency regulation", *IET Gener. Transm. Distrib*, vol. 10, no. 3, pp. 736-749, 2016
- [21] P. A. A. Osman, A. S. El-wakeel and H. M. Seoudy, "Optimal Tuning of PI Controllers for Doubly-Fed Induction Generator-Based Wind Energy Conversion System using Grey Wolf Optimizer", *J. Eng. Res. Appl*, vol. 5, no. 11, pp. 81-87, 2015.
- [22] Z. Civelek, E. Çam, M. Lüy and H. Mamur, "Proportional-integral-derivative parameter optimisation of blade pitch controller in wind turbines by a new intelligent genetic algorithm", *IET Renew. Power Gener*, vol. 10, no. 8, pp. 1220-1228, 2016.
- [23] M. Medeiros Rocha, J. Patrocinio da Silva and F. das Chagas Barbosa de Sena, "Simulation of a Fuzzy Control Applied to a Variable Speed Wind System Connected to the Electrical Network," in *IEEE Latin America Transactions*, vol. 16, no. 2, pp. 521-526, Feb. 2018.
- [24] Ganthia, B.P., Barik, S.K. Steady-State and Dynamic Comparative Analysis of PI and Fuzzy Logic Controller in Stator Voltage Oriented Controlled DFIG Fed Wind Energy Conversion System. *J. Inst. Eng. India Ser. B*101,273–286 (2020). <https://doi.org/10.1007/s40031-020-00455-8>.
- [25] Ganthia, B. P., Barik, S. K., Nayak, B., "Shunt Connected FACTS Devices for LVRT Capability Enhancement in WECS", *Engineering, Technology & Applied Science Research*, 10(3), pp. 5819-5823.
- [26] Bibhu Prasad Ganthia, "Application of Hybrid Facts Devices in DFIG Based Wind Energy System for LVRT Capability Enhancements". *Journal of Mechanics of Continua and Mathematical Sciences*. 15. 10.26782/jmcmcs.2020.06.00019.
- [27] B. P. Ganthia, S. Mohanty, P. K. Rana and P. K. Sahu, "Compensation of voltage sag using DVR with PI controller," 2016 International Conference on Electrical, Electronics, and Optimization Techniques (ICEEOT), Chennai, 2016, pp. 2138-2142, doi: 10.1109/ICEEOT.2016.7755068.
- [28] B.P. Ganthia, P.K. Rana, T. Patra, R. Pradhan and R. Sahu, "Design and Analysis of Gravitational Search Algorithm Based TCSC Controller in Power System", *Materials Today: Proceedings*, vol. 5, no. 1, pp. 841-847, 2018.
- [29] A. Honrubia-Escribano, F. Jiménez-Buendía, E. Gómez-Lázaro and J. Fortmann, "Field Validation of a Standard Type 3 Wind Turbine Model for Power System Stability, According to the Requirements Imposed by IEC 61400-27-1," in *IEEE Transactions on Energy Conversion*, vol. 33, no. 1, pp. 137-145, March 2018.
- [30] L. Sun, C. Peng, J. Hu and Y. Hou, "Application of Type 3 Wind Turbines for System Restoration," in *IEEE Transactions on Power Systems*, vol. 33, no. 3, pp. 3040-3051, May 2018.
- [31] Ganthia, Bibhu Prasad and Subrat Kumar Barik, and Byamakesh Nayak. "Comparative Analysis of Various Types of Control Techniques for Wind Energy Conversion System." In *Modeling and Control of Static Converters for Hybrid Storage Systems*. edited by Fekik, Arezki, and NacereddineBenamrouche, 143-174. Hershey, PA: IGI Global, 2022. <http://doi:10.4018/978-1-7998-7447-8.ch006>.

- [32] Ganthia, Bibhu Prasad and Monalisa Mohanty, and Jai Kumar Maherchandani. "Power Analysis Using Various Types of Wind Turbines." In *Modeling and Control of Static Converters for Hybrid Storage Systems*. edited by Fekik, Arezki, and Nacereddine Benamrouche, 271-286. Hershey, PA: IGI Global, 2022. <http://doi:10.4018/978-1-7998-7447-8.ch010>.
- [33] Ganthia B.P., Barik S.K., Nayak B. (2021) Wind Turbines in Energy Conversion System: Types & Techniques. In: Singh V.K., Bhoi A.K., Saxena A., Zobia A.F., Biswal S. (eds) *Renewable Energy and Future Power Systems*. Energy Systems in Electrical Engineering. Springer, Singapore. [https://doi.org/10.1007/978-981-33-6753-1\\_9](https://doi.org/10.1007/978-981-33-6753-1_9)
- [34] Ganthia, B. P., Barik, S. K., Nayak, B., "Hardware in Loop (THIL 402) Validated Type-I Fuzzy Logic Control of Type-III Wind Turbine System under Transients". *J. Electrical Systems*, 17-1 (2021): 28-51. [journal/esrgroups.org/jes](http://journal/esrgroups.org/jes)
- [35] Ö. Göksu, M. Altin, J. Fortmann and P. E. Sørensen, "Field Validation of IEC 61400-27-1 Wind Generation Type 3 Model With Plant Power Factor Controller," in *IEEE Transactions on Energy Conversion*, vol. 31, no. 3, pp. 1170-1178, Sept. 2016.
- [36] D. N. Hussein, M. Matar and R. Iravani, "A Wideband Equivalent Model of Type-3 Wind Power Plants for EMT Studies," in *IEEE Transactions on Power Delivery*, vol. 31, no. 5, pp. 2322-2331, Oct. 2016.
- [37] C. Bhattacharjee and B. K. Roy, "Advanced fuzzy power extraction control of wind energy conversion system for power quality improvement in a grid tied hybrid generation system," in *IET Generation, Transmission & Distribution*, vol. 10, no. 5, pp. 1179-1189, 7 4 2016.
- [38] Mohamed M. Ismail, Ahmed F. Bendary, Protection of DFIG wind turbine using fuzzy logic control, *Alexandria Engineering Journal*, Volume 55, Issue 2, 2016, Pages 941-949.
- [39] D. Lamsal, T. Conradie, V. Sreeram, Y. Mishra and D. Kumar, "Fuzzy-based smoothing of fluctuations in output power from wind and photovoltaics in a hybrid power system with batteries", *International Transactions on Electrical Energy Systems*, vol. 29, no. 3, November 2018.
- [40] D. Ochoa and S. Martinez, "Frequency dependent strategy for mitigating wind power fluctuations of a doubly-fed induction generator wind turbine based on virtual inertia control and blade pitch angle regulation", *Renewable Energy*, vol. 128, pp. 108-124, Dec 2018.
- [41] A. Honrubia-Escribano, F. Jimenez-Buendia, E. Gomez-Lazaro and J. Fortmann, "Field validation of a standard Type 3 wind turbine model for power system stability, according to the requirements imposed by IEC 61400-27-1," 2018 IEEE Power & Energy Society General Meeting (PESGM), Portland, OR, 2018, pp. 1-1.
- [42] S. A. Eisa, W. Stone and K. Wedeward, "Mathematical Modeling, Stability, Bifurcation Analysis, and Simulations of a Type-3 DFIG Wind Turbine's Dynamics with Pitch Control," 2017 Ninth Annual IEEE Green Technologies Conference (GreenTech), Denver, CO, 2017, pp. 334-341.
- [43] B. P. Ganthia, V. Agarwal, K. Rout and M. K. Pardhe, "Optimal control study in DFIG based wind energy conversion system using PI & GA," 2017 International Conference on Power and Embedded Drive Control (ICPEDC), Chennai, 2017, pp. 343-347.
- [44] B. P. Ganthia, S. Mohanty, P. K. Rana and P. K. Sahu, "Compensation of voltage sag using DVR with PI controller," 2016 International Conference on Electrical, Electronics, and Optimization Techniques (ICEEOT), Chennai, 2016, pp. 2138-2142, doi: 10.1109/ICEEOT.2016.7755068.
- [45] Pragati A., Ganthia B.P., Panigrahi B.P. (2021) Genetic Algorithm Optimized Direct Torque Control of Mathematically Modeled Induction Motor Drive Using PI and Sliding Mode Controller. In: Kumar J., Jena P. (eds) *Recent Advances in Power Electronics and Drives*. Lecture Notes in Electrical Engineering, vol 707. Springer, Singapore. [https://doi.org/10.1007/978-981-15-8586-9\\_32](https://doi.org/10.1007/978-981-15-8586-9_32)
- [46] Siraj, Kiran, Haris Siraj, and Mashood Nasir. "Modeling and control of a doubly fed induction generator for grid integrated wind turbine." *Power Electronics and Motion Control Conference and Exposition (PEMC)*, 2014 16th International. IEEE, 2014.
- [47] A. N. Gogdare, A. Doroudi and M. Ghaseminejad, "A new method to mitigate voltage fluctuation of a fixed speed wind farm using DFIG wind turbine," 2012 Proceedings of 17th Conference on Electrical Power Distribution, Tehran, 2012, pp. 1-6.
- [48] Ganthia B.P., Pradhan R., Sahu R., Pati A.K. (2021) Artificial Ant Colony Optimized Direct Torque Control of Mathematically Modeled Induction Motor Drive Using PI and Sliding Mode Controller. In: Kumar J., Jena P. (eds) *Recent Advances in Power Electronics and Drives*. Lecture Notes in Electrical Engineering, vol 707. Springer, Singapore. [https://doi.org/10.1007/978-981-15-8586-9\\_35](https://doi.org/10.1007/978-981-15-8586-9_35)
- [49] Subash Ranjan Kabat, Chinmoy Kumar Panigrahi, Bibhu Prasad Ganthia, Fuzzy Logic Based Fault Current Prediction in Double Fed Induction Generator Based Wind Turbine System, *Materials Today: Proceedings*, 2021, ISSN 2214-7853, <https://doi.org/10.1016/j.matpr.2021.06.403>.
- [50] Bibhu Prasad Ganthia *et al* 2022 *J. Phys.: Conf. Ser.* 2161 012066.
- [51] Satpathy S.R., Pradhan S., Pradhan R., Sahu R., Biswal A.P., Ganthia B.P. (2021) Direct Torque Control of Mathematically Modeled Induction Motor Drive Using PI-Type-I Fuzzy Logic Controller and Sliding Mode Controller. In: Udgata S.K., Sethi S., Srirama S.N. (eds) *Intelligent Systems*. Lecture Notes in Networks and Systems, vol 185. Springer, Singapore. [https://doi.org/10.1007/978-981-33-6081-5\\_2](https://doi.org/10.1007/978-981-33-6081-5_2).
- [52] Sthitprajna Mishra *et al* 2022 *J. Phys.: Conf. Ser.* 2161 012068.

- [53] Sidhartha Kumar Samal *et al* 2022 *J. Phys.: Conf. Ser.* 2161 012069.
- [54] Fu, Y., Kumar, J., Ganthia, B.P. *et al.* Nonlinear dynamic measurement method of software reliability based on data mining. *Int J Syst Assur Eng Manag* (2021). <https://doi.org/10.1007/s13198-021-01389-0>.
- [55] Xie, Hui, Wang, Yatao, Gao, Zhiliang, Ganthia, Bibhu Prasad and Truong, Chinh V. "Research on frequency parameter detection of frequency shifted track circuit based on nonlinear algorithm" *Nonlinear Engineering*, vol. 10, no. 1, 2021, pp. 592-599. <https://doi.org/10.1515/nleng-2021-0050>.
- [56] Gu, Ji, Wang, Wei, Yin, Rong, Truong, Chinh V and Ganthia, Bibhu Prasad. "Complex circuit simulation and nonlinear characteristics analysis of GaN power switching device" *Nonlinear Engineering*, vol. 10, no. 1, 2021, pp. 555-562. <https://doi.org/10.1515/nleng-2021-0046>.
- [57] Dr. Rambabu Chunduri, Benisha Gracelin , Dr. Dishore ShunmughamVanaja,Subhashree Priyadarshini, Aradhana Khillo,Bibhu Prasad Ganthia, "Design and Control of a Solar Photovoltaic Fed Asymmetric Multilevel Inverter Using Computational Intelligence", *Annals of RSCB*, vol. 25, no. 6, pp. 17731–17743, Jul. 2021.
- [58] M. Sivaramkrishnan, P. Ramesh, M. Veerasundaram, Lizi Joseph, Bibhu Prasad Ganthia, Dr. M. Anand, "Ann Based Speed Control of Brush less DC Motor Using DC DC Converter", *DE*, pp. 1998 - 2011, Jun. 2021.
- [59] Dr. S. Kaliappan, Dr. V. Parimala, Akshay S., N. Praneeth, Bibhu Prasad Ganthia, Dr. Makarand Upadhyaya, "Bridgeless Ac/Dc Converter & Dc-Dc Based Power Factor Correction with Reduced Total Harmonic Distortion", *DE*, pp. 2012 - 2018, Jun. 2021.
- [60] Dr. V. Parimala, P. V. Ashwathy Devraj, Dr. S. Siva Subramanian, Dr. Udayakumar Durairaj, Bibhu Prasad Ganthia, Dr. Makarand Upadhyaya, "Matlab/Simulink Based THD Reduction Using Active Power Filters ", *DE*, pp. 1990 - 1997, Jun. 2021.